

---

# Regularized Kernel and Neural Sobolev Descent: Dynamic MMD Transport

---

Youssef Mroueh, Tom Sercu and Anant Raj  
IBM Research and MPI  
mroueh@us.ibm.com, tom.sercu1@ibm.com

## Abstract

We introduce Regularized Kernel and Neural Sobolev Descent for transporting a source distribution to a target distribution along smooth paths of minimum kinetic energy (defined by the Sobolev discrepancy), related to dynamic optimal transport. In the kernel version, we give a simple algorithm to perform the descent along gradients of the Sobolev critic, and show that it converges asymptotically to the target distribution in the MMD sense. In the neural version, we parametrize the Sobolev critic with a neural network with input gradient norm constrained in expectation. We show in theory and experiments that regularization has an important role in favoring smooth transitions between distributions, avoiding large discrete jumps. Our analysis could provide a new perspective on the impact of critic updates on the paths to equilibrium in the GAN setting.

## 1 Introduction

Optimal Transport (OT) theory [1, 2] and its computational aspects [3] are increasingly gaining interest in the machine learning community. The problem of finding an optimal transport map between a source distribution  $\nu_q$  and a target distribution  $\nu_p$  goes back to the seminal work of Monge; in the Monge problem one seeks a bijection  $T$  that minimizes a cost function  $c$ :  $\min_T \left\{ \int c(x, T(x)) d\nu_q : T_{\#}\nu_q = \nu_p \right\}$  where  $T_{\#}$  is the push forward operator that moves the positions of all the points in the support of the measure  $\nu_q$  using  $T$ . The Monge map does not necessarily exist, and moreover the problem is not computationally friendly. Later Kantorovich relaxed the deterministic nature of the Monge problem via a coupling  $\pi$  whose marginals are  $\nu_p$  and  $\nu_q$ :  $\min_{\pi} \left\{ \int c(x, y) d\pi(x, y) : \text{s.t } \nu_p \text{ and } \nu_q \text{ are marginals of } \pi \right\}$ . In the discrete case the Kantorovich relaxation boils down to a linear program, or can be solved with entropic regularization via the so called Sinkhorn algorithm [4]. For example for the particular cost function  $c(x, y) = \|x - y\|_2^2$ , the optimal value for the Kantorovich objective is known as the celebrated Wasserstein 2 distance  $W_2^2(\nu_p, \nu_q)$ . Benamou and Brenier [5] showed later that for this particular cost function the optimal transport problem has a fluid dynamic interpretation known as the dynamic formulation:

$$W_2^2(\nu_p, \nu_q) = \inf_{\varphi_t, q_t} \int_0^1 \int \|V_t(x)\|^2 d\nu_{q_t}(x) dt, \text{ s.t } \frac{\partial q_t(x)}{\partial t} = -\text{div}(q_t V_t(x)) \quad q_0 = q, q_1 = p. \quad (1)$$

The optimal transport problem in this perspective corresponds to finding velocity fields  $V_t$  of minimum *kinetic energy* and a *path of densities*  $q_t$  advecting with those velocities from the initial source density  $q_0 = q$  to the a target density  $q_1 = p$ . The optimal path corresponds to the smallest effort as measured by the cumulative kinetic energy. Moreover this problem can be cast as a convex problem and under some mild assumptions on the densities it provides a unique solution to the Monge problem, by following the optimal path from source to target. The velocities  $V_t$  can be obtained from a gradient of a convex potential. Note that the explicit knowledge of the densities  $p$  and  $q$  is needed to solve the Benamou-Brenier formulation.

This paper follows this dynamic point of view of transport where we wish to find a path of distributions connecting source and target distributions while minimizing some form of *kinetic energy*, but with two practical considerations in mind: 1) we assume we have access only to samples from  $p$  and  $q$ . 2) we would like a scalable method (in sample size, input dimension and time complexity) for finding the velocity fields and for advecting the probability mass along those paths i.e. without solving partial differential equations as in Equation 1. Dynamically transporting distributions by their samples can be seen as a simple proxy to the GAN framework, amenable to analysis without min-max complexities.

To enable tractable computation, we restrict our velocity field to be the gradient of a function in a finite dimensional Reproducing Kernel Hilbert Space (RKHS)  $\mathcal{H}$  with a finite feature map  $\Phi : x \rightarrow \Phi(x) \in \mathbb{R}^m$ , hence with kernel  $k$ ,  $k(x, y) = \langle \Phi(x), \Phi(y) \rangle = \sum_{j=1}^m \Phi_j(x)\Phi_j(y)$ . We use the recently introduced regularized Kernel Sobolev Discrepancy [6] as a way to quantify the *kinetic energy* that we wish to minimize. Working in a RKHS allows us to quantify progress made following paths of minimum regularized Kernel Sobolev discrepancy using the maximum mean discrepancy [7]

$$\text{MMD}(\nu_p, \nu_{q_t}) = \left\| \mathbb{E}_{x \sim \nu_p} \Phi(x) - \mathbb{E}_{x \sim \nu_{q_t}} \Phi(x) \right\|.$$

Following paths defined by these minimum kernelized kinetic energy velocity fields, we obtain convergence:  $\text{MMD}(\nu_p, \nu_{q_t}) \rightarrow 0$  as  $t \rightarrow \infty$ . Hence we refer to our method as regularized Kernel Sobolev Descent or dynamic MMD transport. The roadmap of the paper is the following: Section 2 reviews *Regularized Kernel Sobolev Discrepancy* of [6] that will be the kinetic energy we wish to minimize. Section 3 introduces regularized Kernel Sobolev *Descent* that constructs minimum kinetic energy tunable paths that converge in the MMD sense to the target distribution. We highlight the prominent role of regularization in getting smooth paths. Section 4 discusses connections to dynamic OT [5] and Stein Descent of [8, 9]. In Section 5, we give an algorithm for Kernel Sobolev Descent, and introduce the Neural Sobolev Descent where we parametrize the Sobolev critic with a neural network. We show the validity of our approach on synthetic data, image coloring and shape morphing and how it compares to classic OT algorithms.

## 2 Kernel Sobolev Discrepancy: Kinetic Energy Definition

In this Section we review the Kernel Sobolev Discrepancy introduced recently in [6]. The Kernel Sobolev Discrepancy will be fundamental to our Dynamic MMD transport.

**Sobolev Discrepancy.** The Sobolev discrepancy was introduced recently in the context of Generative Adversarial Networks in Sobolev GAN [10]. We start by defining the Sobolev Discrepancy. Let  $\mathcal{X}$  be a compact space in  $\mathbb{R}^d$  with lipchitz boundary  $\partial\mathcal{X}$ .

**Definition 1** (Sobolev Discrepancy [10, 6]). *Let  $\nu_p, \nu_q$  be two measures defined on  $\mathcal{X}$ . The Sobolev Discrepancy is defined as follows:*

$$\begin{aligned} \mathcal{S}(\nu_p, \nu_q) &= \sup_f \left\{ \mathbb{E}_{x \sim \nu_p} f(x) - \mathbb{E}_{x \sim \nu_q} f(x) : f \in W_0^{1,2}(\mathcal{X}, \nu_q), \mathbb{E}_{x \sim \nu_q} \|\nabla_x f(x)\|^2 \leq 1 \right\} \\ &= \inf_f \left\{ \sqrt{\int_{\mathcal{X}} \|\nabla_x f(x)\|^2 d\nu_q(x) : f|_{\partial\mathcal{X}} = 0, p(x) - q(x) = -\text{div}(q(x)\nabla_x f(x))} \right\} \end{aligned}$$

where  $W_0^{1,2}(\mathcal{X}, \nu_q) = \{f \text{ vanishes at the boundary of } \mathcal{X} \text{ and } \mathbb{E}_{x \sim \nu_q} \|\nabla_x f(x)\|^2 < \infty\}$ .

**Remark 1.** We refer to  $\nu_p$  as the target distribution, and  $\nu_q$  as the source distribution. The Sobolev discrepancy finds a witness function (or critic) that maximizes the mean discrepancy between the source and target distribution, while constraining the witness function gradients semi-norm to be in a weighted Sobolev ball (under the source distribution  $\nu_q$ ). Note that the sup form (dual) is computationally friendly since it can be optimized using samples from  $p$  and  $q$ . The inf form (primal) sheds light on the physical meaning of this discrepancy: it is the **minimum kinetic energy** needed to advect the mass  $q$  to  $p$ . This interpretation will play a crucial role in Sobolev Descent.

Recently [6] showed that this Sobolev Discrepancy is rooted in the optimal transport literature and is known as the *homegeonous weighted negative Sobolev norm*  $\|\cdot\|_{\dot{H}^{-1}(\nu_q)}$ , [1, 11, 3]. Indeed the weighted negative Sobolev norm is defined as follows, for a any signed measure  $\chi$ :

$$\|\chi\|_{\dot{H}^{-1}(\nu_q)} = \sup_f \left\{ \left| \int_{\mathcal{X}} f(x) d\chi(x) \right| : f \in W_0^{1,2}(\mathcal{X}, \nu_q), \mathbb{E}_{x \sim \nu_q} \|\nabla_x f(x)\|^2 \leq 1 \right\}.$$

As pointed out in [6] it is easy to see that:  $\mathcal{S}(\nu_p, \nu_q) = \|\nu_p - \nu_q\|_{\dot{H}^{-1}(\nu_q)}$ . The norm  $\|\cdot\|_{\dot{H}^{-1}(\nu_q)}$  plays a fundamental role in dynamic optimal transport [5] since it linearizes the Wasserstein  $W_2$  distance:  $W_2(\nu_q, \nu_q + \varepsilon\chi) = \varepsilon \|\chi\|_{\dot{H}^{-1}(\nu_q)} + o(\varepsilon)$ . For more details on the Sobolev Discrepancy and its connection to optimal transport we refer the reader to [6] and references there in.

**Regularized Kernel Sobolev Discrepancy (RKSD).** In order to define our dynamic MMD transport we need to introduce a last ingredient: the Kernelized Sobolev Discrepancy. In other words a kernelized measure of *minimum kinetic energy for transporting  $q$  to  $p$* .

**RKHS Properties and Assumptions.** Let  $\mathcal{H}$  be a *finite dimensional RKHS* with a finite feature map  $\Phi : x \rightarrow \Phi(x) \in \mathbb{R}^m$ , hence with Kernel  $k$ ,  $k(x, y) = \langle \Phi(x), \Phi(y) \rangle = \sum_{j=1}^m \Phi_j(x)\Phi_j(y)$ , where  $\langle \cdot, \cdot \rangle$  is the dot product in  $\mathbb{R}^m$ . Note that for a function  $f \in \mathcal{H}$ ,  $f(x) = \langle \mathbf{f}, \Phi(x) \rangle$ , where  $\mathbf{f} \in \mathbb{R}^m$  and  $\|f\|_{\mathcal{H}} = \|\mathbf{f}\|$ . Let  $J\Phi(x) \in \mathbb{R}^{d \times m}$  be the jacobian of  $\Phi$ ,  $[J\Phi]_{a,j}(x) = \frac{\partial}{\partial x_a} \Phi_j(x)$ . We have the following expression of the gradient  $\nabla_x f(x) = (J\Phi(x)\mathbf{f}) \in \mathbb{R}^m$ . Mild assumptions on  $\mathcal{H}$  are required ( $\Phi$  bounded and differentiable (A1), has bounded derivatives (A2), and zero boundary condition on  $\Phi$  (A3)) and can be found in [6].

**Regularized Kernel Sobolev Discrepancy.** The Kernel Sobolev Discrepancy [6] restricts the witness function of the Sobolev discrepancy to a finite dimensional RKHS  $\mathcal{H}$ , with feature map  $\Phi$ . The Regularized Kernel Sobolev Discrepancy further regularizes the critic using Tikhonov regularization.

**Definition 2 (RKSD).** Let  $\mathcal{H}$  be a *finite dimensional RKHS* satisfying assumptions A1, A2 and A3. Let  $\lambda > 0$  be the regularization parameter. Let  $\nu_p, \nu_q$  be two measures defined on  $\mathcal{X}$ . The regularized Kernel Sobolev discrepancy restricted to the space  $\mathcal{H}$  is defined as follows:

$$\mathcal{S}_{\mathcal{H}, \lambda}(\nu_p, \nu_q) = \sup_{f \in \mathcal{H}} \left\{ \mathbb{E}_{x \sim \nu_p} f(x) - \mathbb{E}_{x \sim \nu_q} f(x) : \mathbb{E}_{x \sim \nu_q} \|\nabla_x f(x)\|^2 + \lambda \|f\|_{\mathcal{H}}^2 \leq 1 \right\} \quad (2)$$

We identify in the constraint in Equation (2) a regularized operator defined by  $D(\nu_q) = \mathbb{E}_{x \sim \nu_q} ([J\Phi(x)]^\top J\Phi(x))$ . The constraint can be written as  $\langle \mathbf{f}, D(\nu_q) + \lambda I_m \mathbf{f} \rangle \leq 1$ . Following [6] we call  $D(\nu_q)$  the Kernel Derivative Gramian Embedding (KDGE) of  $\nu_q$ . KDGE is an operator embedding of the distribution. The KDGE can be seen as ‘‘covariance’’ of the jacobian. This operator embedding of  $\nu_q$  is to be contrasted with the classic Kernel Mean Embedding (KME) of a distribution,  $\mu(\nu_q) = \mathbb{E}_{x \sim \nu_q} \Phi(x)$ .

The following proposition proved in [6] summarizes properties of the squared RKSD :

**Proposition 1** (Closed Form Expression of RKSD). Let  $\lambda > 0$ . We have:

$\mathcal{S}_{\mathcal{H}, \lambda}^2(\nu_p, \nu_q) = \sup_{\mathbf{u} \in \mathbb{R}^m} 2 \langle \mathbf{u}, \mu(\nu_p) - \mu(\nu_q) \rangle - \langle \mathbf{u}, (D(\nu_q) + \lambda I_m) \mathbf{u} \rangle$ . This has the following closed form:  $\mathcal{S}_{\mathcal{H}, \lambda}^2(\nu_p, \nu_q) = \left\| (D(\nu_q) + \lambda I_m)^{-\frac{1}{2}} (\mu(\nu_p) - \mu(\nu_q)) \right\|^2$  and the optimal witness function  $u_{p,q}^\lambda$  of  $\mathcal{S}_{\mathcal{H}, \lambda}^2(\nu_p, \nu_q)$  satisfies:  $u_{p,q}^\lambda(x) = \langle \mathbf{u}_{p,q}^\lambda, \Phi(x) \rangle$  where:  $(D(\nu_q) + \lambda I_m) \mathbf{u}_{p,q}^\lambda = \mu(\nu_p) - \mu(\nu_q)$ . Note that  $\mathcal{S}_{\mathcal{H}, \lambda}^2(\nu_p, \nu_q) = \int_{\mathcal{X}} \|\nabla_x u_{p,q}^\lambda(x)\|^2 q(x) dx + \lambda \|\mathbf{u}_{p,q}^\lambda\|^2$  is the minimum regularized kinetic energy for advecting  $q$  to  $p$  using gradients of potentials in  $\mathcal{H}$ .

**Remark 2.** a) From this proposition we see that  $\nabla_x u_{p,q}^\lambda(x)$  can be seen as velocities of minimum regularized kinetic energy, advecting  $q$  to  $p$ . b) We give here the expression of the witness function  $u_{p,q}^\lambda$  of  $\mathcal{S}_{\mathcal{H}, \lambda}^2(\nu_p, \nu_q)$  rather than  $\mathcal{S}_{\mathcal{H}, \lambda}(\nu_p, \nu_q)$  for convenience. The witness in (2) is  $u_{p,q}^\lambda / \mathcal{S}_{\mathcal{H}, \lambda}$ .

**Empirical RKSD.** An estimate of the Sobolev critic given finite samples from  $p$  and  $q$   $\{x_i, i = 1 \dots N, x_i \sim p\}$ , and  $\{y_i, i = 1 \dots M, y_i \sim q\}$  is straightforward:  $\hat{u}_{p,q}^\lambda(x) = \langle \hat{\mathbf{u}}_{p,q}^\lambda, \Phi(x) \rangle_{\mathbb{R}^m}$ , where  $\hat{\mathbf{u}}_{p,q}^\lambda = (\hat{D}(\hat{\nu}_q) + \lambda I_m)^{-1} (\hat{\mu}(\hat{\nu}_p) - \hat{\mu}(\hat{\nu}_q))$ . With the empirical KDGE is given by  $\hat{D}(\hat{\nu}_q) = \frac{1}{M} \sum_{j=1}^M [J\Phi(y_j)]^\top J\Phi(y_j)$ , and the empirical KMEs  $\hat{\mu}(\hat{\nu}_p) = \frac{1}{N} \sum_{i=1}^N \Phi(x_i)$  and  $\hat{\mu}(\hat{\nu}_q) = \frac{1}{M} \sum_{j=1}^M \Phi(y_j)$ .

### 3 Regularized Kernel Sobolev Descent: Paths of minimum Kinetic Energy

Now that we have a notion of Kernelized kinetic energy (the RKSD) and velocity fields consisting in the gradients of the Sobolev critic that achieve the minimum kinetic energy for advecting a source to a target distribution, we are now ready to introduce the Sobolev Descent. Our goal is to construct an infinitesimal transport map  $T^\varepsilon$  of the source distribution  $\nu_q$ , so that the resulting distribution  $\nu_{q[T^\varepsilon]}$

gets close to the target distribution  $\nu_p$  in the MMD sense. For  $x \sim \nu_q$ , moving along the gradient flow of the optimal regularized Sobolev critic  $u_{p,q}^\lambda$  results in a decrease in MMD. We will show that, using the infinitesimal transport map:  $T^\varepsilon(x) = x + \varepsilon \nabla_x u_{p,q}^\lambda(x)$ ,  $x \sim \nu_q$ , the push forward  $T_{\#} \nu_q = \nu_{q[T^\varepsilon]}$  ensures that:  $\text{MMD}(\nu_p, \nu_{q[T^\varepsilon]}) \leq \text{MMD}(\nu_p, \nu_q)$ .

**MMD as a Functional over probabilities and its First variation.** In order to characterize the variation in the MMD distance under small perturbations of the source distribution, we think of the MMD as a functional over the probability space  $\mathcal{P}(\mathcal{X})$ . The following definition of the first variation of functionals over Probability is a fundamental tool in our analysis. The reader is referred to [2, Chapter 7] for more context on first variations and gradient flows in optimal transport.

**Definition 3** (First variation of Functionals over Probability). *We shall fix in the following a measure  $\nu_p$  and perturb  $\nu_q$  with a perturbation  $\chi$  so that  $\nu_q + \varepsilon \chi$  belongs to  $\mathcal{P}(\mathcal{X})$  for small  $\varepsilon$  (We have necessarily  $\int d\chi = 0$ ). Let  $F$  be a functional:  $\mathcal{P}(\mathcal{X}) \times \mathcal{P}(\mathcal{X}) \rightarrow \mathbb{R}^+$ . We treat  $F(\nu_p, \nu_q)$ , as a functional over probability in its second argument and compute its first variation as follows:*

$$\left. \frac{d}{d\varepsilon} F(\nu_p, \nu_q + \varepsilon \chi) \right|_{\varepsilon=0} = \lim_{\varepsilon \rightarrow 0} \frac{F(\nu_p, \nu_q + \varepsilon \chi) - F(\nu_p, \nu_q)}{\varepsilon} := \int \frac{\delta F}{\delta \nu_q}(\nu_p, \nu_q) d\chi.$$

Hence the following elementary Lemma on the first variation of the MMD distance:

**Lemma 1** (Perturbation of  $\text{MMD}^2$ , First variation). *Recall that  $\text{MMD}^2(\nu_p, \nu_q) = \|\mu(\nu_p) - \mu(\nu_q)\|^2 = \|\mathbb{E}_{x \sim \nu_p} \Phi(x) - \mathbb{E}_{x \sim \nu_q} \Phi(x)\|^2$ . We have the following first variation for the MMD distance:*

$$\left. \frac{d}{d\varepsilon} \text{MMD}^2(\nu_p, \nu_q + \varepsilon \chi) \right|_{\varepsilon=0} = -2 \int \delta_{p,q}(x) d\chi(x), \text{ where } \delta_{p,q}(x) = \langle \mu(\nu_p) - \mu(\nu_q), \Phi(x) \rangle.$$

**From infinitesimal transport maps to small perturbations.** Let  $\psi \in \mathcal{H}$ , following [9] we consider infinitesimal transport maps:  $T^\varepsilon(x) = x + \varepsilon \nabla_x \psi(x)$ ,  $x \sim \nu_q$ . Let  $q$  be the density of  $X$  we are interested in the density  $q_{T^\varepsilon}$  of  $T^\varepsilon(X)$  as  $\varepsilon \rightarrow 0$ . Consider  $\varepsilon$  small so that  $\nabla T^\varepsilon(x) = I + \varepsilon H\psi(x)$  is positive definite, where  $H$  is the hessian matrix of  $\psi$  (i.e  $\varepsilon < \sup_{x \in \mathcal{X}} \frac{1}{|\lambda_{\max}(H\psi(x))|}$ ). Therefore we have:  $(T^\varepsilon)^{-1}(x) = x - \varepsilon \nabla_x \psi(x) + o(\varepsilon)$ . A first order expansion gives us:

$$\begin{aligned} q_{[T^\varepsilon]}(x) &= q((T^\varepsilon)^{-1}(x)) \det(\nabla_x (T^\varepsilon)^{-1}(x)) \\ &= (q(x) - \varepsilon \langle \nabla_x q(x), \nabla_x \psi(x) \rangle) \det(I - \varepsilon \nabla_x^2 \psi(x)) + o(\varepsilon) \\ &= (q(x) - \varepsilon \langle \nabla_x q(x), \nabla_x \psi(x) \rangle) (1 - \text{trace}(\varepsilon \nabla_x^2 \psi(x))) + o(\varepsilon) \\ &= q(x) - \varepsilon (\langle \nabla_x q(x), \nabla_x \psi(x) \rangle + q(x) \Delta \psi(x)) + o(\varepsilon) \\ &= q(x) - \varepsilon (\text{div}(q(x) \nabla_x \psi(x))) + o(\varepsilon) \end{aligned}$$

Hence we are interested in perturbation of the form  $d\chi(x) = -\text{div}(q(x) \nabla_x \psi(x)) dx$ , since it is the first order variation of the density as we transport points distributed as  $\nu_q$  using the infinitesimal transport map  $T^\varepsilon$ , for small  $\varepsilon$ . Note that  $\int_{\mathcal{X}} d\chi(x) = 0$ .

**Transport using the gradient flows of the regularized Sobolev Critic.** The following theorem specializes Lemma 1 to the perturbation induced by the regularized Sobolev critic  $\psi = u_{p,q}^\lambda$ , i.e for  $d\chi_u(x) = -\text{div}(q(x) \nabla_x u_{p,q}^\lambda(x)) dx$ .

**Theorem 1** (Gradient flows of the Regularized Sobolev Critic decreases the MMD distance). *Let  $\lambda > 0$ . Let  $u_{p,q}^\lambda$  be the solution of the regularized Kernel Sobolev discrepancy between  $\nu_p$  and  $\nu_q$  i.e  $u_{p,q}^\lambda = (D(\nu_q) + \lambda I_m)^{-1}(\mu(\nu_p) - \mu(\nu_q))$ . Consider  $d\chi_u(x) = -\text{div}(q(x) \nabla_x u_{p,q}^\lambda(x)) dx$ , i.e corresponding to the infinitesimal transport of  $\nu_q$  via  $T^\varepsilon(x) = x + \varepsilon \nabla_x u_{p,q}^\lambda(x)$ . We have the following first variation of the  $\text{MMD}^2$  under this particular perturbation:*

$$\left. \frac{d}{d\varepsilon} \text{MMD}^2(\nu_p, \nu_q + \varepsilon \chi_u) \right|_{\varepsilon=0} = -2 (\text{MMD}^2(\nu_p, \nu_q) - \lambda \mathcal{S}_{\mathcal{H}, \lambda}^2(\nu_p, \nu_q)) \leq 0.$$

**Remark 3.** *The  $\leq 0$  of the RHS above is guaranteed since for any  $\lambda > 0$  we have  $\mathcal{S}_{\mathcal{H}, \lambda}^2(\nu_p, \nu_q) \leq \|(D(\nu_q) + \lambda I)^{-1/2}\|_{\text{op}}^2 \|\mu(\nu_p) - \mu(\nu_q)\|^2 \leq \frac{1}{\lambda} \text{MMD}^2(\nu_p, \nu_q)$  (where  $\|\cdot\|_{\text{op}}$  is the operator norm).*



From this Theorem we conclude that the transform  $T^\varepsilon(x) = x + \varepsilon \nabla_x u_{p,q}^\lambda(x)$  i.e using the gradient flows of the regularized Sobolev critic, results in a decrease in the MMD, i.e by moving the mass along the gradients of the Sobolev critic (i.e velocities of minimum regularized kinetic energy), we make progress towards matching  $p$  in the MMD sense. The amount of progress made is proportional to  $(\text{MMD}^2(\nu_p, \nu_q) - \lambda \mathcal{S}_{\mathcal{H}, \lambda}^2(\nu_p, \nu_q)) := \Delta_q$ .

Theorem 1 suggests an iterative procedure that transports a source distribution  $\nu_q$  to a target distribution  $\nu_p$ : we start with applying transform  $T_0^\varepsilon(x) = x + \varepsilon \nabla_x u_{p,q_0}^\lambda(x)$  on  $q = q_0$  which decreases the squared MMD distance by  $\Delta_{q_0}$ . This results in a new distribution  $q_1(x) = q_0[T_0^\varepsilon](x)$ . To further decrease the MMD distance we apply a new transform on  $q_1$ ,  $T_1^\varepsilon(x) = x + \varepsilon \nabla_x u_{p,q_1}^\lambda(x)$ ; this results in a decrease of the squared MMD distance by  $\Delta_{q_1}$ . By iterating this process we construct a path of distributions  $\{q_\ell\}_{\ell=0 \dots L-1}$  between  $q_0$  and  $p$ :

$$q_{\ell+1} = q_\ell[T_\ell^\varepsilon] \text{ where } T_\ell^\varepsilon(x) = x + \varepsilon \nabla_x u_{p,q_\ell}^\lambda(x), x \sim \nu_{q_\ell}. \quad (3)$$

We call this iterative process Sobolev Descent, and this incremental decrease in the MMD distance is summarized in the following corollary:

**Corollary 1** (Regularized Sobolev Descent Decreases the MMD). *Consider the path of distributions  $q_\ell$  between  $q_0 = q$  and  $p$  constructed in equation (3) we have for  $\ell \in \{0, \dots, L-1\}$ :*

$$\left. \frac{d}{d\varepsilon} \text{MMD}^2(\nu_p, \nu_{q_\ell}) \right|_{\varepsilon=0} = -2 (\text{MMD}^2(\nu_p, \nu_{q_\ell}) - \lambda \mathcal{S}_{\mathcal{H}, \lambda}^2(\nu_p, \nu_{q_\ell})) \leq 0.$$

*Proof.* By Theorem 1, noting that for small  $\varepsilon$  we have:  $q_{\ell+1}(x) = q_\ell(x) - \varepsilon \text{div}(q_\ell(x) \nabla_x u_{p,q_\ell}^\lambda(x))$ .  $\square$

**The important role of regularization in Sobolev Descent: Regularization as a damping favoring smoother distribution paths.** Note that the magnitude of the decrease in the MMD distance is controlled by the magnitude of the regularized Kernel Sobolev Discrepancy and the regularization parameter  $\lambda$ . Hence  $\lambda$  controls the smoothness of the transitions in the path of distributions  $q_\ell$ . Note that we have two cases:

*Case 1:  $\lambda = 0$ , Unregularized Sobolev Discrepancy Flows.* Assume that  $D(\nu_q)$  is non singular. Let us consider the continuous descent defined for  $t = \varepsilon$  and note  $\nu_{q_t}$  the measure at time  $t$ , as  $\varepsilon \rightarrow 0$ . Hence Corollary 1 suggests the following dynamic of the MMD :

$$\frac{d}{dt} \text{MMD}^2(\nu_p, \nu_{q_t}) = -2 \text{MMD}^2(\nu_p, \nu_{q_t}).$$

This suggests a fast exponential convergence of  $\nu_{q_t}$  to  $\nu_p$  in the MMD sense:  $\text{MMD}^2(\nu_p, \nu_{q_t}) = e^{-2t} \text{MMD}^2(\nu_p, \nu_{q_0})$ , i.e  $\text{MMD}^2(\nu_p, \nu_{q_t}) \rightarrow 0$ , as  $t \rightarrow \infty$ . This fast convergence is not necessarily desirable as it may imply non-smooth paths with large discrete jumps from  $q_0$  to  $p$ . For instance  $q_t(x) = (1 - e^{-t})p(x) + e^{-t}q_0(x)$  exhibits this type of exponential convergence, but corresponds to intermediate distributions that are trivial interpolations between source and target distributions, and don't correspond to a meaningful smooth path from source to target, in the spirit of the Benamou-Brenier dynamic transport. See Figure 1 for an illustration.

*Case 2:  $\lambda > 0$  Regularized Sobolev Discrepancy Flows.* In this case Corollary 1 suggests the following non linear dynamic of the MMD :

$$\frac{d}{dt} \text{MMD}^2(\nu_p, \nu_{q_t}) = -2 (\text{MMD}^2(\nu_p, \nu_{q_t}) - \lambda \mathcal{S}_{\mathcal{H}, \lambda}^2(\nu_p, \nu_{q_t})) \leq 0.$$

While the MMD still decreases and  $\text{MMD}^2(\nu_p, \nu_{q_t}) \rightarrow 0$  as  $t \rightarrow \infty$ , the regularization slows down the convergence by a factor proportional to the regularized Sobolev discrepancy  $\lambda \mathcal{S}_{\mathcal{H}, \lambda}^2(\nu_p, \nu_{q_t})$ . Therefore regularization here is not only playing a computational role that stabilizes computation, it is also playing the role of a *damping* that slows down the convergence of  $\nu_{q_t}$  to the target distribution  $\nu_p$ . This *damping* is desirable as it favors smoother paths between  $q_0$  and  $p$ , i.e paths that deviates from the exponential regime in the un-regularized case. Hence we obtain tunable paths via regularization that favors smoother transitions from source to target (See Figure 1).

**Remark 4.** Let  $(\lambda_j, d_j)$  be eigenvalues and eigenvectors of  $D(\nu_q)$ . It is easy to see that:  $\nabla_x u_{p,q}^\lambda(x) = \sum_{j=1}^m \frac{1}{\lambda_j + \lambda} \langle d_j, \mu(\nu_p) - \mu(\nu_q) \rangle \nabla_x d_j(x)$ , where  $\nabla_x d_j(x) = [J\Phi(x)]d_j$ . One can think of  $\nabla_x d_j(x)$  as **principal transport directions** [6]. Regularization is introducing therefore a spectral filter on principal transport directions by weighing down directions with low eigenvalues. Those directions imply high frequency motions resulting in discrete jumps and discontinuous paths, filtering them out ensures smoother transitions in the probability path. More details in Appendix B.

## 4 Relation to Previous Work

Dynamic OT of Benamou-Brenier [5] and Stein descent [9] are the closest to Sobolev Descent. The Benamou-Brenier formulation and Sobolev Descent minimize two related forms of kinetic energy ( $\|\cdot\|_{\dot{H}^{-1}(\nu_q)}$  and  $\mathcal{S}_{\mathcal{H},\lambda}^2$ ) in order to find paths connecting source and target distributions. The main differences are in the assumptions on the densities, the definition of the kinetic energy and the velocity fields that minimize it, and in the paths they define. Table 1 summarizes those main differences (and see Appendix C for an illustration). In the stein method [12–16], one of the measures  $\nu_p$  is assumed to have a known density function  $p$  and we would like to measure the fidelity of samples from  $\nu_q$  to the likelihood of  $p$ . The Stein discrepancy is obtained by applying a differential operator  $T(p)$  to a vector valued function  $\varphi : \mathcal{X} \rightarrow \mathbb{R}^d$ , where  $T(p)\varphi(x) = \langle \nabla_x \log(p(x)), \varphi(x) \rangle + \text{div}(\varphi(x))$ . The Kernelized Stein Discrepancy is defined as follows:  $\mathbb{S}(\nu_p, \nu_q) = \sup_{\varphi} \{\mathbb{E}_{x \sim \nu_q} T(p)\varphi(x) : \varphi_j \in \mathcal{H}, \sum_{j=1}^d \|\varphi_j\|_{\mathcal{H}}^2 \leq 1\}$ . Let  $\varphi_{p,q}^*$  be the optimal solution. Variational Stein Descent of [9] uses  $\varphi_{p,q}^*$  as a velocity field to transport particles distributed according to  $\nu_q$  to approximate the target  $\nu_p$ . This construct paths reducing the KL divergence [8] (no explicit kinetic energy being minimized).

	Densities	Kinetic Energy (KE) and Velocities	Paths
Benamou Brenier [5]	$p, q$ known	KE between $q_t$ and $q_t + dq_t$ Min KE = $\ dq_t\ _{\dot{H}^{-1}(q_t)}^2$ Min KE = $\int_{\mathcal{X}} \ V_t^*(x)\ ^2 q_t(x) dx$ Velocity $V_t^*$ from critic of $\ dq_t\ _{\dot{H}^{-1}(q_t)}^2$	Optimal Paths minimizing KE between time steps $T_{\#}(\nu_q) = \nu_p$ , $W_2^2(p, q) = \int_0^1 \ dq_t\ _{\dot{H}^{-1}(q_t)}^2 dt$
Stein Descent [9, 8]	$p$ known samples $\sim q$	KE between $q_t$ and $p$ Velocity $\varphi_{p,q_t}^*(x)$ $\varphi_{p,q_t}^* \in \mathcal{H}^d$ critic of $\mathbb{S}^2(p, q_t)$ KE = $\int_{\mathcal{X}} \ \varphi_{p,q_t}^*(x)\ ^2 q_t(x) dx$ (not min)	Paths minimizing KL divergence between $q_t$ and target $p$ $\lim_{t \rightarrow \infty} \text{KL}(q_t, p) = 0$
Reg. Sobolev Descent (This work)	samples $\sim p$ samples $\sim q$	KE between $q_t$ and $p$ Min Reg KE = $\mathcal{S}_{\mathcal{H},\lambda}^2(p, q_t)$ = $\int_{\mathcal{X}} \ \nabla_x u_{p,q}^\lambda\ ^2 q_t(x) dx + \lambda \ u_{p,q_t}^\lambda\ _{\mathcal{H}}^2$ Velocity $\nabla_x u_{p,q_t}^\lambda(x)$ $u_{p,q_t}^\lambda \in \mathcal{H}$ critic of $\mathcal{S}_{\mathcal{H},\lambda}^2(p, q_t)$	Tunable paths via $\lambda$ minimizing Reg. KE between $q_t$ and target $p$ $\lim_{t \rightarrow \infty} \text{MMD}(q_t, p) = 0$

Table 1: Comparison with Benamou-Brenier and Stein Descent.

## 5 Algorithms and Experiments

**Algorithms.** We specify here the regularized Sobolev Descent for empirical measures  $\hat{\nu}_p$  and  $\hat{\nu}_q$ , given finite samples from  $p$  and  $q$ :  $\{x_i, i = 1 \dots N, x_i \sim p\}$ , and  $\{y_i, i = 1 \dots M, y_i \sim q\}$ .

**Remark 5.** *Assumption (A3) on zero boundary condition can be weakened to  $q(x) \langle \nabla_x u_{p,q}^\lambda(x), n(x) \rangle = 0$  on  $\partial\mathcal{X}$  ( $n(x)$  is the normal on  $\partial\mathcal{X}$ ). Assuming  $\mathcal{X} = \mathbb{R}^d$  and that  $q$  and  $p$  vanish at  $\infty$  we can use non vanishing feature maps  $\Phi$  on  $\partial\mathcal{X}$ .*

**Empirical Regularized Kernel Sobolev Descent with Random Fourier Features.** We consider the finite dimensional RKHS induced by random Fourier features [17] ( $\Phi(x) = \cos(Wx + b)$ ,  $W_{ij} \sim \mathcal{N}(0, 1/\sigma^2)$ ,  $b_i \sim \text{Unif}[0, 2\pi]$ ). The empirical descent consists in using the estimate  $\hat{u}_{p,q}^\lambda$  in Equation (3). For  $\varepsilon > 0$ , we have the following iteration, for  $\ell \geq 1$  and all current positions of source particles  $i = 1, \dots, M$ :  $x_i^\ell = x_i^{\ell-1} + \varepsilon \nabla_x \hat{u}_{p,q_{\ell-1}}^\lambda(x_i^{\ell-1})$  with  $\hat{\nu}_{q_{\ell-1}}(dx) = \frac{1}{M} \sum_{i=1}^M \delta(x - x_i^{\ell-1}) dx$ , the empirical measure of particles  $\{x_i^{\ell-1}, i = 1 \dots M\}$ , initialized with source particles  $\{x_i^0 = y_i, i = 1 \dots M\}$ , and  $\hat{u}_{p,q_{\ell-1}}^\lambda$  is the optimal critic of the empirical RKSD between empirical measure  $\hat{\nu}_p$  and  $\hat{\nu}_{q_{\ell-1}}$ . The empirical regularized Kernel Sobolev Descent can be written as follows: for  $l = \{1 \dots L\}$ :  $\hat{u}_{p,q_{\ell-1}}^\lambda = (\hat{D}(\hat{\nu}_{q_{\ell-1}}) + \lambda I_m)^{-1} (\hat{\mu}(\hat{\nu}_p) - \hat{\mu}(\hat{\nu}_{q_{\ell-1}}))$  and  $x_i^\ell = x_i^{\ell-1} + \varepsilon [J\Phi(x_i^{\ell-1})] \hat{u}_{p,q_{\ell-1}}^\lambda, \forall i = 1, \dots, M$ . The Empirical Sobolev Descent is summarized in Algorithm 1, and the smoothness of the paths is controlled via the regularization parameter  $\lambda$ .

**Neural Sobolev Descent.** Inspired by the success of Sobolev GAN [10] that uses neural network approximations to estimate the Sobolev critic, we propose the Neural Sobolev Descent. In Neural Sobolev Descent the critic function between  $\nu_{q_t}$  and  $\nu_p$  is estimated using a Neural Network  $f_\xi(x) = \langle v, \Phi_\omega(x) \rangle$ , where  $\xi = (v, \omega)$  are the parameters of the neural network that we learn by gradient descent. We follow [10] in optimizing the parameters of the critic via an augmented Lagrangian. The

particles descent is the same as in the Kernelized Sobolev Descent. Note that gradient descent on the parameters of the critic between updates of the particles is initialized with previous parameters (warm restart). Neural Sobolev Descent is summarized in Algorithm 2. Note that when compared to Sobolev GAN this descent replaces the generator with particles. It is worth mentioning that regularization in the neural context is obtained via early stopping, i.e the number of updates  $n_c$  of the critic. Early stopping is known as a regularizer for gradient descent [18]. We will see that the smoothness of the distribution paths is controlled via  $n_c$ .

**Experiments.** We confirm our theoretical findings on regularized Sobolev descent on a synthetic example highlighting the crucial role of regularization in smooth paths convergence. We then baseline Sobolev descent versus classical OT algorithms on the image color transfer problem. We show well-behaved trajectories of Sobolev descent in shape morphing thanks to smooth regularized paths.

**Synthetic 1D Gaussians.** Figure 1 shows Sobolev descent trajectories on a toy 1D problem, where both source and target are 1D Gaussians. Note that the Benamou-Brenier solution would be a *smooth* trajectory of normal distributions, where both the mean and standard deviation linearly interpolate between  $q_0$  and  $p$ . Given 1000 samples from  $q_0$  and  $p$ , we show in Figure 1 results of both kernel and neural Sobolev descent, where we plot kernel density estimators of densities at various time steps in the descent. We show the results of the descent for varying capacity of the function space ( $\sigma$  for the random features kernel, number of layers for Neural), and various regularization parameters ( $\lambda$  Tikhonov regularization for Kernel and  $n_c$  early stopping for Neural). Column (a) shows a regularized low capacity model achieving good approximation of the Benamou-Brenier optimal trajectory, where the data remains concentrated and smoothly moves to the target distribution. Column (b) shows a higher capacity model which blurs out the distribution before converging to  $p$ , where column (c) we even further decrease the regularization (smaller  $\lambda$ , bigger  $n_c$ ) confirming the undesirable interpolation behavior which is predicted by the theory in the un-regularized case. Note that even in the Neural SD case this happens, corresponding to high frequency critic gradient behavior. In column (d) we increase the regularization on the high capacity model, achieving again a behavior that is closer to the optimal, without blurring or interpolation. This confirms the damping effect of regularization, filtering out the high frequency gradients. This can be also seen in the MMD plot in the last column. Figure 8 in Appendix E.2 gives similar results on the morphing task.

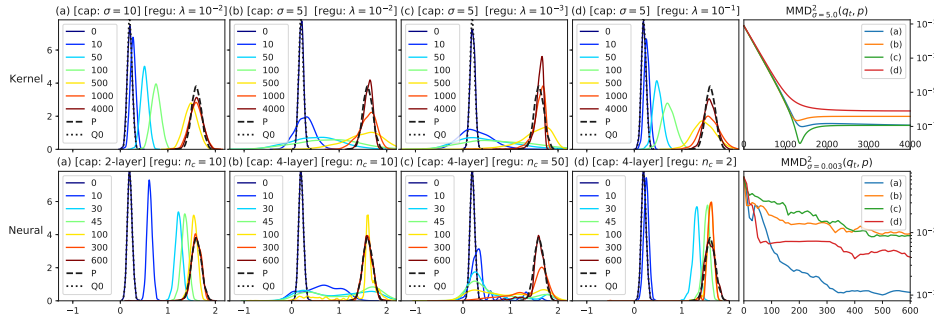


Figure 1: Moving 1000 samples of a 1D gaussian  $\nu_{q_0} = \mathcal{N}(0.2, \sigma = 0.005)$  to  $\nu_p = \mathcal{N}(1.6, \sigma = 0.1)$  with Kernel (top row) and Neural (bottom row) Sobolev Descent. Columns have similar properties between kernel and neural variants in terms of capacity of the model and regularization of the descent: (a) low capacity, (b) high capacity, (c) high capacity with decreased regularization and (d) high capacity with increased regularization.

**Image Color Transfer.** We consider the task of image color manipulation where we would like for an image  $A$  to match the color distribution of an image  $B$ . More formally, consider colored images Source and Target which we see as defining 3-dimensional probability distributions  $\nu_{q_0}$  and  $\nu_p$ , where every pixel is a sample:  $\{x_1, x_2, \dots, x_N\} \sim \nu_{q_0}$  and  $\{y_1, y_2, \dots, y_N\} \sim \nu_p$  and  $N = 256 \times 256 = 66k$  the resolution. We move the samples using Kernel Sobolev Descent and Neural Sobolev Descent and analyze the distributions  $q_t$ . We provide in Figure 2 the results of our proposed algorithm on the task of image color transfer, comparing against results obtained with static Optimal Transport<sup>1</sup>. We show scatter plots after subsampling 5k points at random and display them on the (R,B) channels. In Appendix E Figures 6 and 7 we show the final MMD in function of rbf bandwidth  $\sigma$  and the evolution of the  $q_t$  distribution during the descent.

<sup>1</sup>We follow the recipe of [19] as implemented in the POT library [20] where we subsample for computational feasibility, then use interpolation for out-of-sample points.

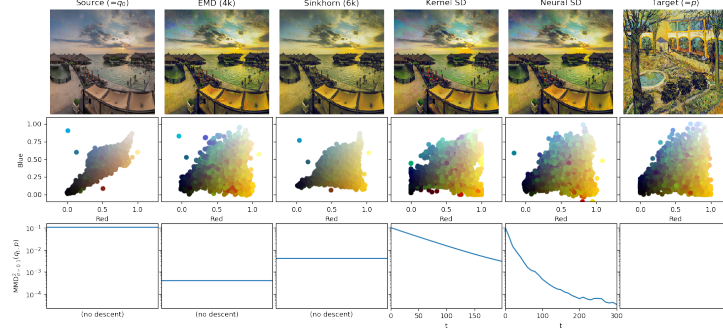


Figure 2: Color transfer. We compare Earth Mover Distance solved with linear programming on 4k samples, Sinkhorn on 6k samples with regularization  $\varepsilon = 1e^{-2}$ , Kernel SD with  $\lambda = 1e^{-2}$  and  $\sigma = 0.1$  at  $t = 200$ , and Neural SD at  $t = 300$ . The bottom row shows progress during the descent by computing the  $\text{MMD}(\nu_{q_t}, \nu_p)$  with bandwidth  $\sigma = 0.1$  using 300 random Fourier features. Neural descent has a clear computational advantage over OT alternatives, which alleviates the need for subsampling and out of sample interpolation (which explains the high MMD values even for EMD).

**Shape Morphing with Sobolev Descent.** We consider here the application of Sobolev descent for morphing between shapes. The source distribution is a uniform distribution on a shape  $A$ , that we need to morph to become shape  $B$ . Such type of morphing or displacement interpolations has been considered in the Wasserstein Barycenter framework [21, 22]. Figure 3 shows the result of Kernelized Sobolev Descent (Algorithm 1) transforming between a source shape  $\nu_q$  and a target shape  $\nu_p$ , using random fourier features for  $m = 100$  and  $L = 600$ ,  $\varepsilon = 0.01$  and  $\lambda = 0.01$ . We see that Kernelized Sobolev Descent morphs the shapes as the number of iterations approaches  $L = 600$ . Figure 4 shows Neural Sobolev Descent morphing between source shapes and target shapes. The first column is the source shape and last column is the target shape, in between columns are intermediate outputs of the Neural Sobolev Descent. Neural Sobolev Descent converges even on complex and unrelated shapes. Appendix E.3 provides the implementation and training details, and visualizes the critic  $f_\xi(x)$  during the descent (Figure 9). Code is available on <https://bit.ly/2GtWXsY>. Videos of shapes morphing are available on <https://goo.gl/X4o8v6>.

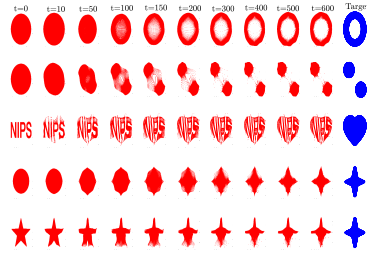


Figure 3: Morphing between several shapes using Kernelized Sobolev Descent. Intermediate steps are intermediate particles states of the Sobolev descent. Last column in the output of Kernelized Sobolev Descent.

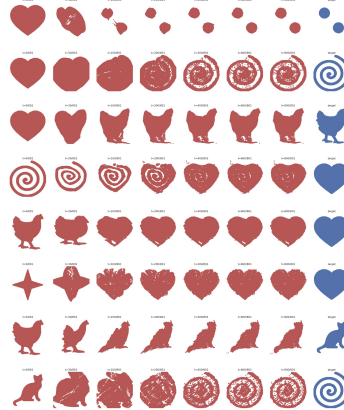


Figure 4: Morphing between several shapes using Neural Sobolev Descent. The descent is performed using a critic modeled by a simple 3-layer MLP.

## 6 Conclusion

We introduced regularized Kernel and Neural Sobolev Descent, as dynamic MMD transport of distributions. We highlighted the crucial role of regularization in obtaining smooth transition paths from source to target, inhibiting large discrete jumps through high frequency gradients. Our work sheds some light on gradient based learning of GANs such as Sobolev GAN [10], that can be seen as a dynamic transport rather than the static transport point of view popularized by WGAN [23]. Stabilization in the GAN context through early stopping (small critic updates) has been empirically observed [24, 25]. Our analysis could provide a new angle on the interaction between critic updates and how GAN reaches an equilibrium.

**Acknowledgements:** The authors thank two of the anonymous ICML reviewers that helped improving the paper.

## References

- [1] Cédric Villani. *Optimal Transport: Old and New*. Grundlehren der mathematischen Wissenschaften. Springer, 2008.
- [2] Filippo Santambrogio. Optimal transport for applied mathematicians. May 2015.
- [3] Gabriel Peyré and Marco Cuturi. Computational optimal transport. Technical report, 2017.
- [4] Marco Cuturi. Sinkhorn distances: Lightspeed computation of optimal transport. In *Advances in neural information processing systems*, pages 2292–2300, 2013.
- [5] Jean-David Benamou and Yann Brenier. A computational fluid mechanics solution to the Monge-Kantorovich mass transfer problem. *Numerische Mathematik*, 2000.
- [6] Youssef Mroueh. Regularized finite dimensional kernel sobolev discrepancy. *Tech Rep. arXiv:1805.06441*, 2018.
- [7] Arthur Gretton, Karsten M. Borgwardt, Malte J. Rasch, Bernhard Schölkopf, and Alexander Smola. A kernel two-sample test. *JMLR*, 2012.
- [8] Qiang Liu. Stein variational descent as a gradient flow. *NIPS*, 2017.
- [9] Qiang Liu and Dilin Wang. Stein variational gradient descent: A general purpose bayesian inference algorithm. In *Advances in Neural Information Processing Systems 29*. 2016.
- [10] Youssef Mroueh, Chun-Liang Li, Tom Sercu, Anant Raj, and Yu Cheng. Sobolev gan. *ICLR*, 2018.
- [11] Rémi Peyre. Comparison between  $w_2$  distance and  $h$ - norm, and localisation of wasserstein distance. 2016.
- [12] Jackson Gorham and Lester W. Mackey. Measuring sample quality with stein’s method. In *NIPS*, pages 226–234, 2015.
- [13] Qiang Liu, Jason D. Lee, and Michael I. Jordan. A kernelized stein discrepancy for goodness-of-fit tests. In *Proceedings of the 33rd International Conference on Machine Learning, ICML 2016, New York City, NY, USA, June 19-24, 2016*, 2016.
- [14] Kacper Chwialkowski, Heiko Strathmann, and Arthur Gretton. A kernel test of goodness of fit. In *ICML 2016*, 2016.
- [15] Jack Gorham, Andrew B. Duncan, Sebastian J. Vollmer, and Lester W. Mackey. Measuring sample quality with diffusions. *CoRR*, abs/1611.06972, 2016.
- [16] Jackson Gorham and Lester W. Mackey. Measuring sample quality with kernels. In *ICML*, 2017.
- [17] Ali Rahimi and Benjamin Recht. Random features for large-scale kernel machines. In *NIPS*. 2008.
- [18] Yuan Yao, Lorenzo Rosasco, and Andrea Caponnetto. On early stopping in gradient descent learning. *Constructive Approximation*, 2007.
- [19] Sira Ferradans, Nicolas Papadakis, Julien Rabin, Gabriel Peyré, and Jean-François Aujol. Regularized discrete optimal transport. In *International Conference on Scale Space and Variational Methods in Computer Vision*, 2013.
- [20] Rémi Flamary and Nicolas Courty. Pot python optimal transport library. 2017.

- [21] Justin Solomon, Fernando de Goes, Gabriel Peyré, Marco Cuturi, Adrian Butscher, Andy Nguyen, Tao Du, and Leonidas Guibas. Convolutional wasserstein distances: Efficient optimal transportation on geometric domains. *ACM Trans. Graph.*, 2015.
- [22] Marco Cuturi and Arnaud Doucet. Fast computation of wasserstein barycenters. In *ICML*, 2014.
- [23] Martin Arjovsky, Soumith Chintala, and Leon Bottou. Wasserstein gan. *Arxiv*, 2017.
- [24] Martin Arjovsky and Léon Bottou. Towards principled methods for training generative adversarial networks. In *ICLR*, 2017.
- [25] William Fedus, Mihaela Rosca, Balaji Lakshminarayanan, Andrew M Dai, Shakir Mohamed, and Ian Goodfellow. Many paths to equilibrium: Gans do not need to decrease adivergence at every step. *arXiv preprint arXiv:1710.08446*, 2017.
- [26] Tadahisa Funaki. A certain class of diffusion processes associated with nonlinear parabolic equations. *Zeitschrift für Wahrscheinlichkeitstheorie und Verwandte Gebiete*, 1984.

## A Algorithm

---

### Algorithm 1 Empirical Kernelized Sobolev Descent

---

**Inputs:**  $\varepsilon$  Learning rate,  $L$  number of iterations  
 $\{x_i, i = 1 \dots N\}$ , drawn from target distribution  $\nu_p$ ,  $\{y_j, j = 1 \dots M\}$  drawn from source distribution  $\nu_q$   $\mathcal{H}$  a Hypothesis Class  
**Initialize**  $x_j^0 = y_j, j = 1 \dots M$   
**for**  $\ell = 1 \dots L$  **do**  
    **Critic Update**  
    Compute Sobolev Critic in  $\mathcal{H}$ , between  $q_{\ell-1}$  and  $p$   
 $\hat{\mathbf{u}}_{p,q_{\ell-1}}^\lambda = \left( \hat{D}(\hat{\nu}_{q_{\ell-1}}) + \lambda I_m \right)^{-1} (\hat{\boldsymbol{\mu}}(\hat{\nu}_p) - \hat{\boldsymbol{\mu}}(\hat{\nu}_{q_{\ell-1}}))$   
    **Particles Update**  
    **for**  $j = 1$  **to**  $M$  **do**  
         $x_j^\ell = x_j^{\ell-1} + \varepsilon \nabla_x \hat{\mathbf{u}}_{p,q_{\ell-1}}^\lambda(x_j^{\ell-1})$  ( $q_\ell$  is the density of the particles  $x_j^\ell$ )  
    **end for**  
**end for**  
**Output:**  $\{x_j^T, j = 1 \dots M\}$

---



---

### Algorithm 2 Neural Sobolev Descent (ALM Algorithm)

---

**Inputs:**  $\varepsilon$  Learning rate particles,  $n_c$  number of critics updates,  $L$  number of iterations  
 $\{x_i, i = 1 \dots N\}$ , drawn from target distribution  $\nu_p$   
 $\{y_j, j = 1 \dots M\}$  drawn from source distribution  $\nu_q$   
Neural critic  $f_\xi(x) = \langle v, \Phi_\omega(x) \rangle$ ,  $\xi = (v, \omega)$  parameters of the neural network  
**Initialize**  $x_j^0 = y_j, j = 1 \dots M$   
**for**  $\ell = 1 \dots L$  **do**  
    **Critic Update**  
    (between particles updates gradient descent on the critic is initialized from previous episodes)  
    **for**  $j = 1$  **to**  $n_c$  **do**  
         $\hat{\mathcal{E}}(\xi) \leftarrow \frac{1}{N} \sum_{i=1}^N f_\xi(x_i) - \frac{1}{M} \sum_{j=1}^M f_\xi(x_j^{\ell-1})$   
         $\hat{\Omega}(\xi) \leftarrow \frac{1}{M} \sum_j \|\nabla_x f_\xi(x_j^{\ell-1})\|^2$   
         $\mathcal{L}_S(\xi, \lambda) = \hat{\mathcal{E}}(\xi) + \lambda(1 - \hat{\Omega}(\xi)) - \frac{\rho}{2}(\hat{\Omega}(\xi) - 1)^2$   
         $(g_\xi, g_\lambda) \leftarrow (\nabla_\xi \mathcal{L}_S, \nabla_\lambda \mathcal{L}_S)(\xi, \lambda)$   
         $\xi \leftarrow \xi + \eta \text{ADAM}(\xi, g_\xi)$   
         $\lambda \leftarrow \lambda - \rho g_\lambda$  {SGD rule on  $\lambda$  with learning rate  $\rho$ }  
    **end for**  
    **Particles Update**  
    **for**  $j = 1$  **to**  $M$  **do**  
         $x_j^\ell = x_j^{\ell-1} + \varepsilon \nabla_x f_\xi(x_j^{\ell-1})$  (current  $f_\xi$  is the critic between  $q_{\ell-1}$  and  $p$ )  
    **end for**  
**end for**  
**Output:**  $\{x_j^T, j = 1 \dots M\}$

---

## B Regularization as smoothing of Principal Transport Directions.

In order to further understand the role of regularization let us take a close look on the expression of the Sobolev critic. Let  $(\lambda_j, \mathbf{d}_j), j = 1 \dots m$  be Eigen system the KDGE  $D(\nu_q)$ . We have:  $\mathbf{u}_{p,q}^\lambda = (D(\nu_q) + \lambda I)^{-1}(\boldsymbol{\mu}(\nu_p) - \boldsymbol{\mu}(\nu_q)) = \sum_{j=1}^m \frac{1}{\lambda_j + \lambda} \langle \mathbf{d}_j, \boldsymbol{\mu}(\nu_p) - \boldsymbol{\mu}(\nu_q) \rangle \mathbf{d}_j$ . It follows that  $\nabla_x \mathbf{u}_{p,q}^\lambda(x) = \sum_{j=1}^m \frac{1}{\lambda_j + \lambda} \langle \mathbf{d}_j, \boldsymbol{\mu}(\nu_p) - \boldsymbol{\mu}(\nu_q) \rangle \nabla_x \mathbf{d}_j(x)$ , where  $\nabla_x \mathbf{d}_j(x) = [J\Phi(x)] \mathbf{d}_j$  and  $J\Phi(x) \in \mathbb{R}^{d \times m}$  is the jacobian of  $\Phi$ ,  $[J\Phi]_{a,j}(x) = \frac{\partial}{\partial x_a} \Phi_j(x)$ . One can think of  $\nabla_x \mathbf{d}_j(x)$  as *principal transport directions*. Regularization is introducing therefore a spectral filter on the principal transport directions by weighing down directions with low eigenvalues  $\frac{1}{\lambda_j + \lambda} \approx \frac{1}{\lambda}$  for  $\lambda_j < \lambda$ , and

$\frac{1}{\lambda_j + \lambda} \approx \frac{1}{\lambda_j}$  otherwise. Principal transport directions with small eigenvalues contribute to the fast exponential convergence and may result in discontinuous paths. Regularization filters out those directions, resulting in smoother probability paths between  $\nu_q$  and  $\nu_p$ .

### C Illustration of Sobolev Descent versus dynamic OT

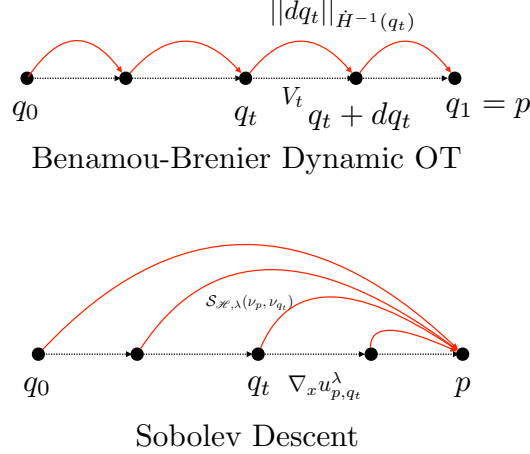


Figure 5: Both formulations minimize a form of kinetic energy, represented with red arrows. While this energy is between consecutive timesteps for dynamic OT (Benamou-Brenier), it is between the current distribution and the target for Sobolev Descent. The velocity fields are represented with dashed arrows, and can be expressed through gradients of a convex potential for dynamic OT. For Sobolev Descent, the velocity fields are the gradient of the Sobolev Critic.

### D Proofs

**Definition 4** (First variation of Functionals over Probability). *We shall fix in the following a measure  $\nu_p$  and perturb  $\nu_q$  with a perturbation  $\chi$  so that  $\nu_q + \varepsilon\chi$  belongs to  $\mathcal{P}(\mathcal{X})$  for small  $\varepsilon$  (We have necessarily  $\int d\chi = 0$ ). Let  $F$  be a functional:  $\mathcal{P}(\mathcal{X}) \times \mathcal{P}(\mathcal{X}) \rightarrow \mathbb{R}^+$ . We treat  $F(\nu_p, \nu_q)$ , as a functional over probability in its second argument and compute its first variation as follows:*

$$\left. \frac{d}{d\varepsilon} F(\nu_p, \nu_q + \varepsilon\chi) \right|_{\varepsilon=0} = \lim_{\varepsilon \rightarrow 0} \frac{F(\nu_p, \nu_q + \varepsilon\chi) - F(\nu_p, \nu_q)}{\varepsilon} := \int \frac{\delta F}{\delta \nu_q}(\nu_p, \nu_q) d\chi$$

**Proposition 2** (Perturbation of the MMD). *Let  $\varphi_{p,q}^* = \frac{\mu(\nu_p) - \mu(\nu_q)}{\|\mu(\nu_p) - \mu(\nu_q)\|_{\mathcal{H}}}$  the witness function of the MMD distance:*

$$MMD(\nu_p, \nu_q) = \sup_{\varphi \in \mathcal{H}, \|\varphi\|_{\mathcal{H}} \leq 1} \int_{\mathcal{X}} \varphi d(\nu_p - \nu_q).$$

*We have the following first variation result:*

$$\left. \frac{d}{d\varepsilon} MMD(\nu_p, \nu_q + \varepsilon\chi) \right|_{\varepsilon=0} = - \int \varphi_{p,q}^* d\chi.$$

*Proof.* This result is direction application of Proposition 7.16 in Chapter 7 of Optimal Transport for applied Mathematicians book.  $\square$

**Lemma 2** (Perturbation of MMD<sup>2</sup>). *We have the following first variation for the MMD distance:*

$$\left. \frac{d}{d\varepsilon} MMD^2(\nu_p, \nu_q + \varepsilon\chi) \right|_{\varepsilon=0} = -2 \int \delta_{p,q}(x) d\chi(x),$$

where  $\delta_{p,q}(x) = \langle \mu(\nu_p) - \mu(\nu_q), \Phi(x) \rangle$ .



*Proof.*

$$\text{MMD}^2(\nu_p, \nu_q) = \|\mu(\nu_p) - \mu(\nu_q)\|^2$$

We extend the kernel mean embedding definition here to signed measures  $\chi$  and note:

$$\mu(\chi) = \int_{\mathcal{X}} \Phi(x) d\chi(x).$$

$$\begin{aligned} \text{MMD}^2(\nu_p, \nu_q + \varepsilon\chi) &= \|\mu(\nu_p) - \mu(\nu_q) - \varepsilon\mu(\chi)\|^2 \\ &= \|\mu(\nu_p) - \mu(\nu_q)\|^2 - 2\varepsilon \langle \mu(\nu_p) - \mu(\nu_q), \mu(\chi) \rangle + \varepsilon^2 \|\mu(\chi)\|^2 \\ &= \text{MMD}^2(\nu_p, \nu_q) - 2\varepsilon \langle \delta_{p,q}, \mu(\chi) \rangle + \varepsilon^2 \|\mu(\chi)\|^2 \\ &= \text{MMD}^2(\nu_p, \nu_q) - 2\varepsilon \int_{\mathcal{X}} \delta_{p,q}(x) d\chi(x) + \varepsilon^2 \|\mu(\chi)\|^2, \end{aligned}$$

where we noted,  $\delta_{p,q} = \mu(\nu_p) - \mu(\nu_q)$  and  $\delta_{p,q}(x) = \langle \delta_{p,q}, \Phi(x) \rangle$ . It follows that:

$$\frac{\text{MMD}^2(\nu_p, \nu_q + \varepsilon\chi) - \text{MMD}^2(\nu_p, \nu_q)}{\varepsilon} = -2 \int_{\mathcal{X}} \delta_{p,q}(x) d\chi(x) + \varepsilon \|\mu(\chi)\|_{\mathcal{H}}^2,$$

Taking the limit  $\varepsilon \rightarrow 0$ , we obtain:

$$\left. \frac{d}{d\varepsilon} \text{MMD}^2(\nu_p, \nu_q + \varepsilon\chi) \right|_{\varepsilon=0} = -2 \int_{\mathcal{X}} \delta_{p,q}(x) d\chi(x)$$

□

Let  $\psi \in \mathcal{H}$ , define:

$$T(x) = x + \varepsilon \nabla_x \psi(x), x \sim \nu_q$$

Let  $q$  be the density of  $X$  we are interested in the density  $q_T$  of  $T(X)$  as  $\varepsilon \rightarrow 0$ . Consider  $\varepsilon$  small so that  $\nabla T(x) = I + \varepsilon H\psi(x)$  is positive definite, where  $H$  is the hessian matrix of  $\psi$ . Therefore we have:

$$T^{-1}(x) = x - \varepsilon \nabla_x \psi(x) + o(\varepsilon).$$

A first order expansion gives us:

$$\begin{aligned} q_{[T]}(x) &= q(T^{-1}(x)) \left| \nabla_x T^{-1}(x) \right| \\ &= (q(x) - \varepsilon \langle \nabla_x q(x), \nabla_x \psi(x) \rangle) \det(I - \varepsilon \nabla_x^2 \psi(x)) + o(\varepsilon) \\ &= (q(x) - \varepsilon \langle \nabla_x q(x), \nabla_x \psi(x) \rangle) (1 - \text{trace}(\varepsilon \nabla_x^2 \psi(x))) + o(\varepsilon) \\ &= q(x) - \varepsilon (\langle \nabla_x q(x), \nabla_x \psi(x) \rangle + q(x) \Delta \psi(x)) + o(\varepsilon) \\ &= q(x) - \varepsilon (\text{div}(q(x) \nabla_x \psi(x))) + o(\varepsilon) \end{aligned}$$

Hence we are interested in perturbation of the form  $d\chi(x) = -\text{div}(q(x) \nabla_x \psi(x)) dx$ , since it is the first order variation of the density as we transport points distributed as  $\nu_q$  using the transport map  $T$ , for small  $\varepsilon$ . Note that  $\int_{\mathcal{X}} d\chi(x) = 0$ .

**Theorem 2** ((Thm 1 restated)). *Let  $\lambda > 0$ . Let  $u_{p,q}^\lambda$  the unnormalized solution of the regularized Kernel Sobolev discrepancy between  $\nu_p$  and  $\nu_q$  i.e  $u_{p,q}^\lambda = (D(\nu_q) + \lambda I)^{-1}(\mu(\nu_p) - \mu(\nu_q))$ . Consider  $d\chi_u(x) = -\text{div}(q(x) \nabla_x u_{p,q}^\lambda(x)) dx$ , i.e corresponding to the infinitesimal transport of  $\nu_q$  via  $T(x) = x + \varepsilon \nabla_x u_{p,q}^\lambda(x)$ . We have the following first variation of the  $\text{MMD}^2$  under this particular perturbation:*

$$\left. \frac{d}{d\varepsilon} \text{MMD}^2(\nu_p, \nu_q + \varepsilon\chi_u) \right|_{\varepsilon=0} = -2 (\text{MMD}^2(\nu_p, \nu_q) - \lambda \mathcal{S}_{\mathcal{H},\lambda}^2(\nu_p, \nu_q)) \leq 0.$$

*Proof of Theorem 1.*

$$\begin{aligned}
\frac{1}{2} \frac{d}{d\varepsilon} \text{MMD}^2(\nu_p, \nu_q + \varepsilon \chi_u) \Big|_{\varepsilon=0} &= - \int \delta_{p,q} d\chi_u = - \int_{\mathcal{X}} \delta_{p,q}(x) (-\text{div}(q(x) \nabla_x u_{p,q}^\lambda(x))) dx \\
&= \int_{\mathcal{X}} \delta_{p,q}(x) \text{div}(q(x) \nabla_x u_{p,q}^\lambda(x)) dx \\
&= - \int_{\mathcal{X}} \langle \nabla_x \delta_{p,q}(x), \nabla_x u_{p,q}^\lambda(x) \rangle q(x) dx \text{ (Divergence theorem and zero boundary)} \\
&= - \int_{\mathcal{X}} \delta_{p,q}^\top [J\Phi(x)]^\top J\Phi(x) \mathbf{u}_{p,q}^\lambda q(x) dx \\
&= - \left\langle \delta_{p,q}, \left( \int_{\mathcal{X}} [J\Phi(x)]^\top J\Phi(x) q(x) dx \right) \mathbf{u}_{p,q}^\lambda \right\rangle \\
&= - \langle \delta_{p,q}, \mathbb{E}_{x \sim \nu_q} ([J\Phi(x)]^\top J\Phi(x)) \mathbf{u}_{p,q}^\lambda \rangle \\
&= - \langle \delta_{p,q}, D(\nu_q) \mathbf{u}_{p,q}^\lambda \rangle \text{ (by definition)} \\
&= - \langle \delta_{p,q}, (D(\nu_q) + \lambda I_m - \lambda I_m) \mathbf{u}_{p,q}^\lambda \rangle \\
&= - \langle \delta_{p,q}, (D(\nu_q) + \lambda I_m) \mathbf{u}_{p,q}^\lambda \rangle + \lambda \langle \delta_{p,q}, \mathbf{u}_{p,q}^\lambda \rangle
\end{aligned}$$

Recall that :

$$(D(\nu_q) + \lambda I_m) \mathbf{u}_{p,q}^\lambda = \delta_{p,q},$$

and by definition the regularized Kernel Sobolev Discrepancy we have:

$$\langle \delta_{p,q}, \mathbf{u}_{p,q}^\lambda \rangle = \mathcal{S}_{\mathcal{H},\lambda}^2(\nu_p, \nu_q),$$

Hence replacing the expressions above we obtain:

$$\begin{aligned}
\frac{1}{2} \frac{d}{d\varepsilon} \text{MMD}^2(\nu_p, \nu_q + \varepsilon \chi) \Big|_{\varepsilon=0} &= - \langle \delta_{p,q}, \delta_{p,q} \rangle + \lambda \mathcal{S}_{\mathcal{H},\lambda}^2(\nu_p, \nu_q) \\
&= -\text{MMD}^2(\nu_p, \nu_q) + \lambda \mathcal{S}_{\mathcal{H},\lambda}^2(\nu_p, \nu_q) \\
&= -(\text{MMD}^2(\nu_p, \nu_q) - \lambda \mathcal{S}_{\mathcal{H},\lambda}^2(\nu_p, \nu_q))
\end{aligned}$$

Note that:

$$\begin{aligned}
\mathcal{S}_{\mathcal{H},\lambda}^2(\nu_p, \nu_q) &= \langle \delta_{p,q}, (D(\nu_q) + \lambda I)^{-1} \delta_{p,q} \rangle \leq \| (D(\nu_q) + \lambda I)^{-1} \|_{op} \|\delta_{p,q}\|^2 \\
&\leq \frac{1}{\lambda} \text{MMD}^2(\nu_p, \nu_q),
\end{aligned}$$

It follows that :

$$\text{MMD}^2(\nu_p, \nu_q) - \lambda \mathcal{S}_{\mathcal{H},\lambda}^2(\nu_p, \nu_q) \geq 0$$

and

$$\frac{1}{2} \frac{d}{d\varepsilon} \text{MMD}^2(\nu_p, \nu_q + \varepsilon \chi) \Big|_{\varepsilon=0} = -(\text{MMD}^2(\nu_p, \nu_q) - \lambda \mathcal{S}_{\mathcal{H},\lambda}^2(\nu_p, \nu_q)) \leq 0.$$

□

## D.1 Continuous Regularized Kernel Sobolev Descent

This section gives some more intuition on a continuous form of Sobolev Descent.

**Non linear Fokker Planck and Deterministic McKean Vlasov Processes.** The regularized Kernel Sobolev descent can be seen as a continuous process, written in this primal form:

$$\begin{aligned}
\min_{u_{p,q_t} \in \mathcal{H}, q_t} \int_0^\infty &\left( \int_{\mathcal{X}} \|\nabla_x u_{p,q_t}(x)\|^2 d\nu_{q_t}(x) + \lambda \|u_{p,q_t}\|_{\mathcal{H}}^2 - 2(\mathbb{E}_{x \sim p} u_{p,q_t}(x) - \mathbb{E}_{x \sim \nu_{q_t}} u_{p,q_t}(x)) \right) dt \\
\frac{\partial q_t}{\partial t}(x) &= -\text{div}(q_t(x) \nabla_x u_{p,q_t}(x)), \nu_{q_0} = \nu_q
\end{aligned}$$

This form gives us the interpretation that we are seeking potentials  $u_{p,q_t}$  in the finite dimensional RKHS, that have minimum regularized kinetic energy  $\int_{\mathcal{X}} \|\nabla_x u_{p,q_t}(x)\|^2 d\nu_{q_t}(x) + \lambda \|u_{p,q_t}\|_{\mathcal{H}}^2$  and that advects  $q_t$  to  $p$ . The advection can be seen informally by noting that we want to maximize  $\mathbb{E}_{x \sim p} u_{p,q_t}(x) - \mathbb{E}_{x \sim \nu_{q_t}} u_{p,q_t}(x) = \langle \mathbf{u}_{p,q_t}, \boldsymbol{\mu}(p) - \boldsymbol{\mu}(q_t) \rangle$ , meaning we want  $\mathbf{u}_{p,q_t}$  to be aligned with the correct transport direction from  $q$  to  $p$ . The evolution of the density is then dictated by the non linear fokker planck equation known as the deterministic McKean-Vlasov equation:

$$\frac{\partial q_t}{\partial t}(x) = -\text{div}(q_t(x) \nabla_x u_{p,q_t}(x))$$

The primal form given above is not computational friendly and hence we are using 1) the dual form of the Sobolev Discrepancy and 2) the equivalence between stochastic differential equation in general and the McKean Vlasov process, as summarized below:

$$\begin{aligned} & \sup_{f_{p,q_t} \in \mathcal{H}, q_t} \int_0^\infty (\mathbb{E}_{x \sim p} f_{p,q_t}(x) - \mathbb{E}_{x \sim q_t} f_{p,q_t}(x)) dt \\ & \text{s.t } \mathbb{E}_{x \sim q_t} \|\nabla_x f_{p,q_t}(x)\|^2 + \lambda \|f_{p,q_t}\|_{\mathcal{H}}^2 \leq 1 \\ & u_{p,q_t} = \mathcal{S}_{\mathcal{H}, \lambda}(\nu_p, \nu_{q_t}) f_{p,q_t}^* \\ & dX_t = \nabla_x u_{p,q_t}(X_t) dt \quad X_t \sim \nu_{q_t} \quad X_0 \sim \nu_q \end{aligned}$$

Finite dimensional RKHS Sobolev descent is exploiting this computational friendly formulation:  $u_{p,q_t}$  has a closed form solutions at each time  $t$ . Neural Sobolev Descent is also using this formulation by solving the optimization problem for each  $u_{p,q_t}$  using gradient descent and an augmented lagrangian.

### What happens when considering $\mathcal{H} = W_0^{1,2}$ and no Regularization?

**Theorem 3** (Convergence of the continuous limit of Sobolev Descent). *Consider particles  $X_0$  with density function  $q_0 = q$  the source density. Let  $\nu_p$  be the target measure whose density is  $p$ . Consider the following continuous process:*

$$dX_t = \mathcal{S}(\nu_p, \nu_{q_t}) \nabla_x f_{\nu_p, \nu_{q_t}}^*(x) dt, \quad (4)$$

let  $q_t$  be the density function of particles  $X_t$  and  $f_{\nu_p, \nu_{q_t}}^*$  the optimal Sobolev critic between  $\nu_p$  and  $\nu_{q_t}$  (whose densities are  $p$  and  $q_t$  respectively). We have:

$$q_t(x) = (1 - e^{-t}) p(x) + e^{-t} q(x),$$

The density  $q_t$  of the particles  $X_t$  approaches the target density  $p$ , as  $t \rightarrow \infty$  (therefore as  $t \rightarrow \infty$   $q_t \rightarrow p$ ).

We see therefore that the unregularized theoretical Sobolev descent boils down also to interpolation, hence the crucial role of regularization.

*Proof of Theorem 3.* Let  $f_{\nu_p, \nu_{q_t}}^*$  be the Sobolev critic between  $q_t$  and  $p$ , it satisfies the following PDE (See [10] for instance) :

$$p(x) - q_t(x) = -\mathcal{S}(\nu_p, \nu_{q_t}) \text{div}(q_t(x) \nabla_x f_{\nu_p, \nu_{q_t}}^*(x)), \quad (5)$$

where  $q_t$  is the distribution of the particles moving with the flow:

$$dX_t = \mathcal{S}(\nu_p, \nu_{q_t}) \nabla_x f_{\nu_p, \nu_{q_t}}^*(X_t) dt, \text{ where the density of } X_0 \text{ is given by } q_0(x) = q(x)$$

by non linear fokker planck equation and results on McKean Vlasov processes [26], the distribution  $q_t$  evolves as follows:

$$\frac{\partial}{\partial t} q_t(x) = -\mathcal{S}(\nu_p, \nu_{q_t}) \text{div}(q_t(x) \nabla_x f_{\nu_p, \nu_{q_t}}^*(x)) \quad (6)$$

From Equation (5) and (6) we see that:

$$\frac{\partial}{\partial t} q_t(x) = (p(x) - q_t(x)),$$

in other words:

$$\frac{\partial}{\partial t}(p(x) - q_t(x)) = -(p(x) - q_t(x)),$$

Hence :

$$\begin{aligned} p(x) - q_t(x) &= (p(x) - q_0(x)) e^{-t} \\ &= e^{-t} (p(x) - q(x)) \end{aligned}$$

It follows:

$$q_t(x) = (1 - e^{-t}) p(x) + e^{-t} \underbrace{q_0(x)}_{q_0(x)}$$

therefore as  $t \rightarrow \infty$ ,  $q_t \rightarrow p$ . □

## E Additional Figures of Sobolev Descent for Image color transfer and shape morphing

### E.1 Color Transfer

See Figure 6 and Figure 7.

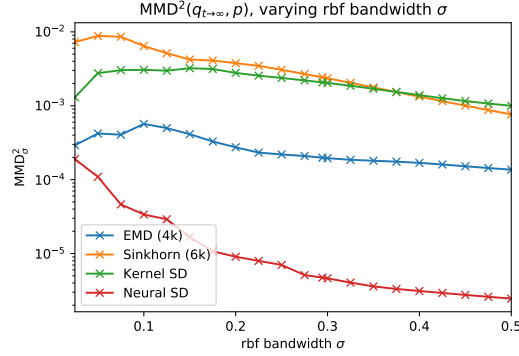


Figure 6: Coloring MMD across a range of rbf bandwidths, using the final  $q_t$  from Figure 2. We select  $\sigma = 0.1$  for the main Figure 2.

### E.2 Shape morphing: Convergence speed

Figure 8 shows MMD convergence for shape morphing with Kernel Sobolev Descent.

### E.3 Shape morphing: Neural Sobolev Descent Level sets and Quiver plots

**Implementation details.** We scaled the input coordinates to be in the  $[-1, 1]$  range. The neural network, implemented in pytorch, is a simple multi-layer perceptron (MLP) with 3 hidden layers (32, 64, 32 respectively), input size 2 and output size 1 ( $= f_\xi(x) \in \mathbb{R}$ ), and Leaky ReLU nonlinearities with negative slope 0.2. We use adam with learning rate  $\eta = 5e^{-4}$  for  $f_\xi$  and  $\varepsilon = 3e^{-3}$ . For penalty weights we have  $\rho = 1e^{-6}$  and initialize with  $\lambda = 0.01$ . We use  $n_c = 10$  (for the first time step we warm up with  $n_c = 50$ ), and run the descent for  $T = 800$  steps. Code is available on <https://goo.gl/tncxQm>. Videos of shapes morphing are available on <https://goo.gl/X4o8v6>.

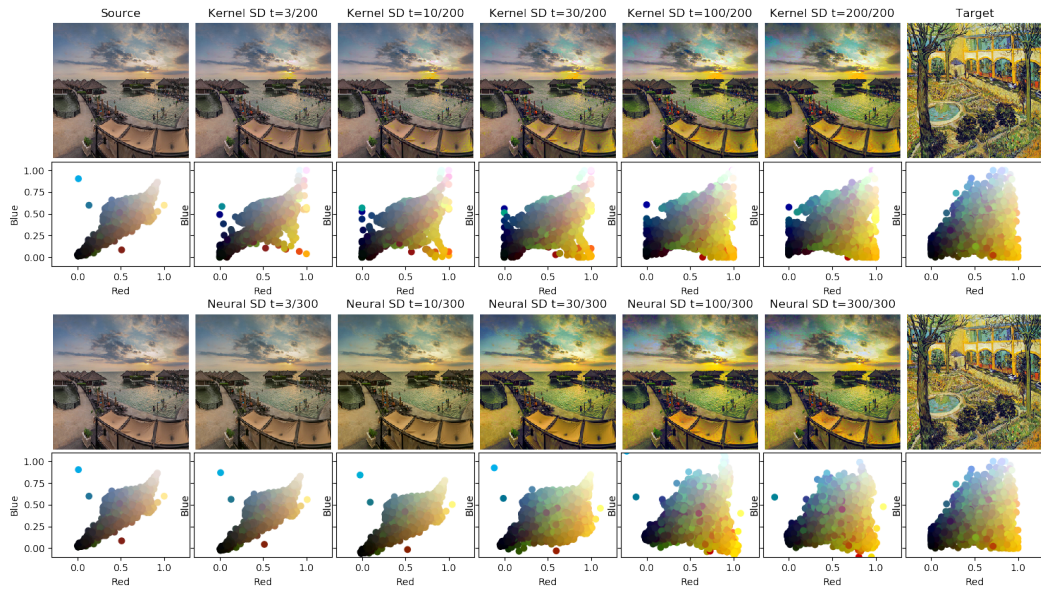


Figure 7: Evolution of  $q_t$  for Kernel and Neural Sobolev Descent.

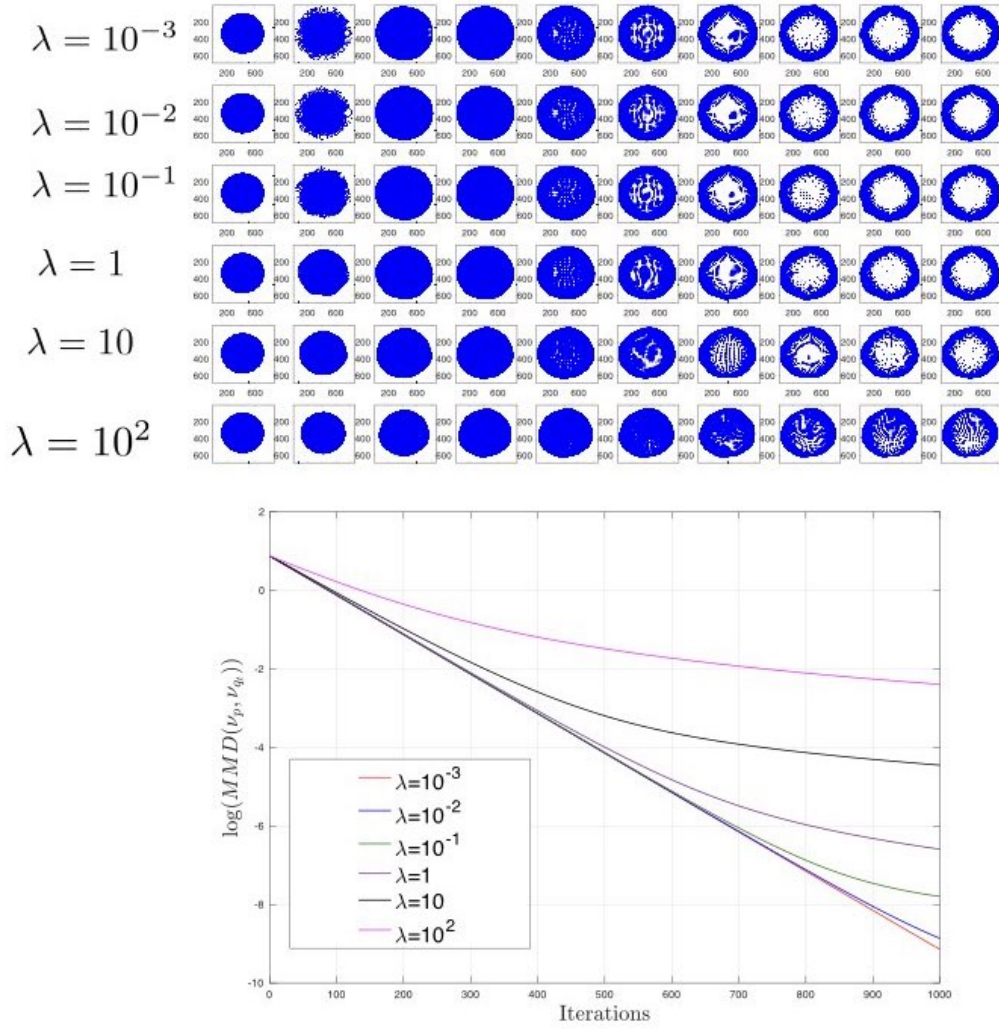


Figure 8: Shape morphing with Kernel Sobolev Descent: We see in this figure that for small regularization the convergence is exponential (linear in log MMD scale). For higher lambda values, regularization slows down the convergence and smooths out the trajectories from  $q$  to  $p$ . We see that for small lambda high frequency motions appearing in early time steps. Those high frequency trajectories are smoothed out with higher regularization, confirming what our theory predicts, on the effect of regularization as a spectral filtering of principal transport direction of the KDGE, favoring smoother distribution paths.

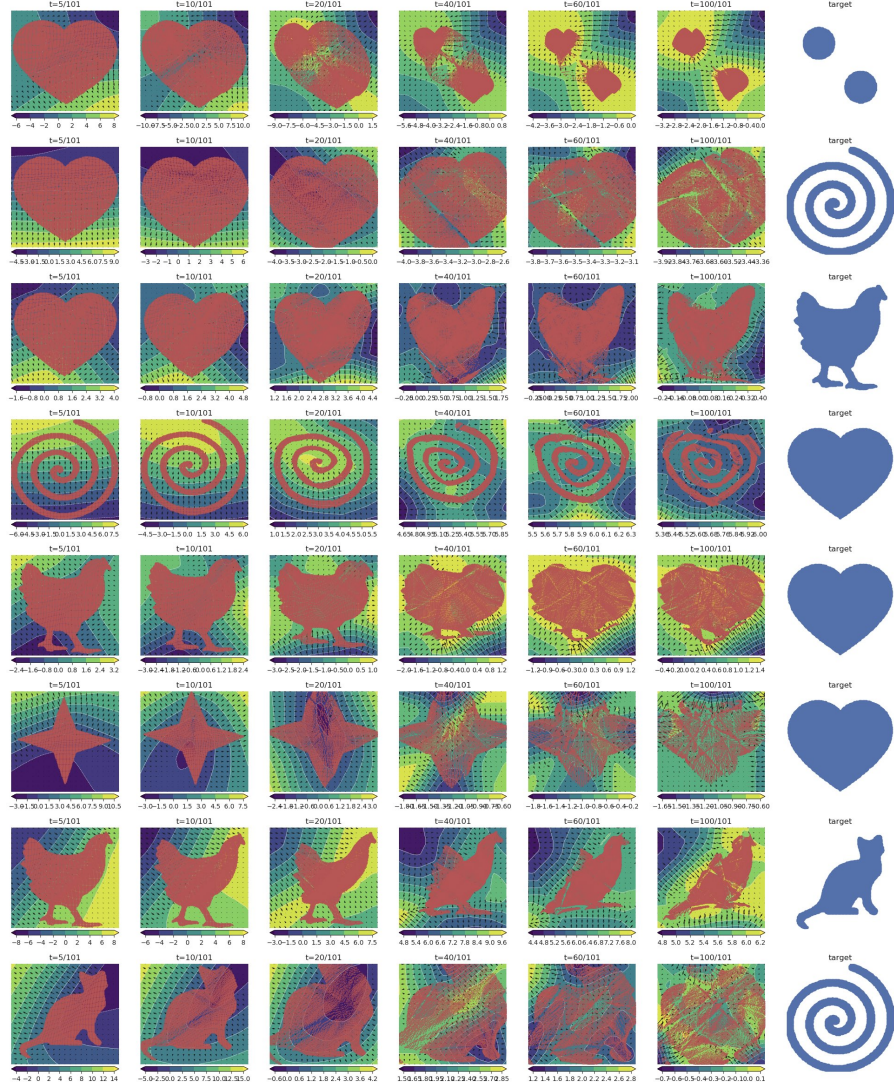


Figure 9: Level sets of  $f_\xi(x)$  and quiver plots showing  $\nabla_x f_\xi(x)$  for the first 100 timesteps of the Neural Sobolev Descent shape morphing results from Figure 4. Videos are available on <https://goo.gl/X4o8v6>.